Science of the Total Environment 952 (2024) 175864

Contents lists available at ScienceDirect

Science of the Total Environment

journal homepage: www.elsevier.com/locate/scitotenv

Microplastic removal and risk assessment framework in a constructed wetland for the treatment of combined sewer overflows

Chiara Sarti [a,b,*], Alessandra Cincinelli [a,c], Riccardo Bresciani [b], Anacleto Rizzo [b], David Chelazzi [c], Fabio Masi [b]

[a] Department of Chemistry "Ugo Schiff", University of Florence, Via della Lastruccia 3, 50019 Sesto Fiorentino, Italy
[b] Iridra Srl, Via La Marmora 51, 50121 Florence, Italy
[c] Department of Chemistry "Ugo Schiff" and CSGI, University of Florence, Via della Lastruccia 3, 50019 Sesto Fiorentino, Italy

HIGHLIGHTS

- Combined sewer overflows (CSOs) are a significant source of microplastics (MPs).
- This is the first study of MP removal in a multi-stage CSO-constructed wetland.
- Microplastic abundance correlates with flow rate and total suspended solids.
- Vertical flow wetland units show higher MP retention than free water surface.
- Ecological risk assessment identified ABS fragments as key high-risk pollutants.

GRAPHICAL ABSTRACT

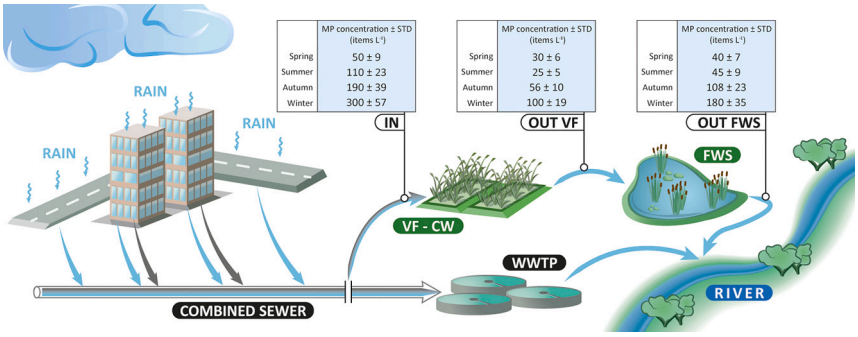

ARTICLE INFO

Keywords:
Microplastics
Plastic polymers
Combined sewer overflow
Nature-based Solution
Constructed Wetland
Treatment Wetland

ABSTRACT

Combined sewer overflows (CSOs) release a significant amount of pollutants, including microplastics (MPs), due to the discharge of untreated water into receiving water bodies. Constructed Wetlands (CWs) offer a promising strategy for CSO treatment and have recently attracted attention as a potential solution for MP mitigation. Nevertheless, limited research on MP dynamics within CSO events and MP removal performance in full-scale CW systems poses a barrier to this frontier of application. This research aims to address both these knowledge gaps, representing the first investigation of a multi-stage CSO-CW for MP removal. The study presents one year of seasonal data from the CSO-CW upstream of the WWTP in Carimate (Italy), evaluating the correlation of MP abundance with different water quality/quantity parameters and associated ecological risks. The results show a clear trend in MP abundance, which increases with rainfall intensity. The strong correlation between MP concentration, flow rate, and total suspended solids (TSS) validates the first flush phenomenon hypothesis and its impact on MP release during CSOs. Chemical characterization identifies acrylonitrile-butadiene-styrene (ABS), polyethylene (PE), and polypropylene (PP) as predominant polymers. The first vertical subsurface flow (VF) stage showed removal rates ranging from 40 % to 77 %. However, the unexpected increase in MP concentrations after the second free water surface (FWS) stage suggests the stochasticity of CSO events and the different hydraulic characteristics of the CW units have diverse effects on MP retention. These data confirm filtration as the

* Corresponding author at: Department of Chemistry "Ugo Schiff", University of Florence, Via della Lastruccia 3, 50019 Sesto Fiorentino, Italy.
E-mail address: chiara.sarti@unifi.it (C. Sarti).

https://doi.org/10.1016/j.scitotenv.2024.175864
Received 14 January 2024; Received in revised form 28 July 2024; Accepted 27 August 2024
Available online 29 August 2024

main retention mechanism for MP within CW systems. The MP ecological risk assessment indicates a high-risk category for most of the water samples, mainly related to the frequent presence of ABS fragments. The results contribute to the current understanding of MPs released by CSOs and provide insights into the performance of different treatment units within a large-scale CSO-CW system, suggesting the requirement for further attention.

1. Introduction

Combined sewers (CSs) are a common infrastructure, designed to transport both domestic and/or industrial wastewater together with urban stormwater runoff (Botturi et al., 2021). Despite modern urban planning favors separate sewers for distinct wastewater types, a significant number of CSs still persist in European countries (Pistocchi et al., 2019). During intense wet weather events, CSs may exceed wastewater treatment plants (WWTPs) conveyance capacity, leading to combined sewer overflows (CSOs) (Quaranta et al., 2022a; Quaranta et al., 2022b). In such instances, the excess wastewater is discharged directly into nearby water bodies through overflow structures, releasing significant amounts of conventional pollutants, pathogens, heavy metals, and emerging microcontaminants (Yu et al., 2022; Masi et al., 2023). Considering the increment of CSO occurrence, caused by climate change and the enhanced soil sealing produced by a growing urbanization (Rizzo et al., 2020), the environmental hazard related to these phenomena is increasing. Therefore, nowadays CSOs can be considered one of the major sources of untreated pollution for aquatic ecosystems (Tondera, 2019; Petrie, 2021).

In particular, CSs serve as a crucial conduit for the migration of terrigenous microplastics (MPs), resulting from both domestic (e.g., washing machines and personal care products) and urban sources (e.g., improper plastic waste disposal and tire abrasion), into receiving water bodies (Mak et al., 2020; Zhou et al., 2023). Generally, in dry weather conditions, MPs generated by urban environments are conveyed through sewer systems to WWTPs, where their removal rates depend on a complex interaction between service area characteristics and treatment processes (Long et al., 2019; Blair et al., 2019). However, intense rainfall events with the consequent surface scouring and CSO occurrences lead to a drastic increase in MP contamination levels for the receiving rivers and estuaries (Liu et al., 2019a; Chen et al., 2020). Despite growing concerns about the global impact of CSOs on aquatic MP pollution, the lack of a comprehensive understanding of MP dynamics within CSO events and their correlation with other water quantity/quality parameters is a significant barrier to the development of targeted mitigation strategies.

Although there is no single effective solution, one of the most promising approaches to reducing the environmental pressure of CSOs can be found in Constructed Wetlands (CWs) (Rizzo et al., 2018), which have proven well-documented removal performances for several classes of contaminants. CW systems offer numerous advantages compared to conventional approaches (e.g., first flush tanks) (Masi et al., 2017), such as a continuous treatment of CSOs, flood protection, increased biodiversity, and recreational opportunities (Rizzo et al., 2021; Perry et al., 2024). Recently, CWs have also been considered as a promising solution for the reduction of MP pollution, although the number of available studies is still limited, especially for large-scale systems (Xu et al., 2022; Liu et al., 2023). An example can be found in the research conducted in Belgium by Wang et al. (2020), who investigated the MP removal efficiency of a horizontal subsurface flow CW (HSF-CW) used as a treatment for WWTP secondary effluents. The result showed a significant reduction in MP concentration, with removal efficiencies of 88 %. Similarly, a MP removal rate equal to 95 % was obtained by Bydalek et al. (2023), who investigated the performance of free water surface (FWS) constructed wetland located in the UK. Furthermore, Wei et al. (2020) assessed the mitigation potential of a subsurface flow CW (SSF-CW) in the Hangzhou region of China. The obtained MP removal rates varied from 45 to 100 %. However, different types of CWs are expected to have diverse interception and adsorption performances, resulting in highly variable MP removal levels (Xu et al., 2022). Furthermore, the combination of various CW designs in large-scale multi-stage CW systems results in a more complex scenario (Zhou et al., 2022). In these treatment processes, the removal mechanism of MPs may show different characteristics, requiring attention and in-depth study. Nonetheless, there is a significant lack of relevant literature on the contribution of large-scale multi-stage CW systems to MP contamination control.

By presenting one year of seasonal data from the CSO-CW upstream of the WWTP in Carimate (Italy), this study aims to address the knowledge gaps on both the occurrence and dynamics of MPs related to CSO events and the potential of CWs for MP control. This research represents, to the best of our knowledge, the first study on MP mitigation with a large-scale multi-stage CSO-CW, providing valuable insights for future developments in CW applications. In particular, the objectives of this study were to: 1) evaluate the occurrence and the physical/chemical characteristics of MPs detected in the water samples collected at three different sampling points of the CSO-CW system; 2) investigate the possible seasonal trends of MP concentration and its correlation with several water quality/quantity parameters to provide a deeper understanding of MP dynamics occurring during CSO events; 3) estimate the MP removal performances obtained by the two CW stages with different designs and hydraulic characteristics for a better comprehension of MP retention mechanisms within CW systems; 4) assess the ecological risk associated with MPs for the receiving water body.

2. Materials and methods

2.1. Case study

The experimental case study is located in Carimate, Italy (45° 42′N, 9° 07′E). The centralized WWTP, managed by the Water Utility Como Acqua Srl, treats wastewater from a combined sewer system serving 11 municipalities in the highly industrialized province of Como, with a total population of 70,040 inhabitants. Upstream of the Carimate WWTP, CSOs are frequent and can persist for long periods, even in dry post-rain conditions.

According to the authorization for discharge into the Seveso River, the WWTP must treat a flow rate of 2700 $m^3\ h^{-1}$ during CSO events. Since the secondary biological treatment can receive a maximum of 2200 $m^3\ h^{-1}$, a CW system, designed by IRIDRA srl, was implemented to treat the excess volume of water. The CW system intercepts part of the diluted pollutant load, estimated at 104 $t_{COD}\ year^{-1}$ (contained in approximately 890,000 $m^3\ year^{-1}$), ensuring compliance with the discharge limits established by Italian legislation (Legislative Decree 152/2006) for the discharge of treated wastewater into freshwater bodies, with limits of 125 mg L^{-1}, 1 mg L^{-1}, 15 mg L^{-1}, and 35 mg L^{-1}, for chemical oxygen demand (COD), total phosphorus (TP), total nitrogen (TN) and total suspended solids (TSS), respectively.

The multistage CW system designed for CSO treatment is described in Fig. 1. The first stage incorporates two vertical subsurface flow (VF) CW beds, each divided into two separate hydraulic sectors (total surface of 8500 m^2), planted with *Phragmites australis*. VF filter media layers are designed as follows (from bottom to top): 15 cm of coarse gravel (Ø 20–40 mm), 15 cm of gravel (Ø 5–10 mm), and 60 cm of pea gravel (Ø 1–5 mm). The second stage consists of a FWS CW (total surface of 4500 m^2) designed with varying water depths (ranging from 0.7 to 1.5 m), to accommodate various autochthonous aquatic plants (*Schenoplectus Lacustris, Menyanthes Trifollata, Typha minima, Nimphea Alba, Lythrum*

Salicaria, Nuphar lutea, Iris Pseudacorus, Carex riparia, Typha latifolia, and Pesicria Amphibia), promoting biodiversity and thus increasing the number of removal pathways and mechanisms for the different pollutants.

The specifics of the Carimate WWTP and further technical details on the CSO-CW system, including the water quantity and quality dataset results of a 3-year monitoring campaign, were extensively discussed by Masi et al. (2023).

2.2. Sample collection

Water samples were collected during 4 different sampling campaigns, one representative of each season (spring, summer, autumn, and winter) of 2022, in three different points of the multi-stage CW system, as highlighted in Fig. S1: influent (IN); effluent from the 1st stage VF CW (OUT VF); effluent from the 2nd stage FWS (OUT FWS). Two samples were collected at each sampling point and analyzed in triplicate in the subsequent laboratory phase to ensure the reliability of the data.

Unlike conventional WWTP or CW systems, the sampling phase represents a considerable challenge for CSO-CWs. As highlighted by Botturi et al. (2021), one of the major criticisms of CSO management is the lack of legislation and harmonized protocols. In general, systematic monitoring of CSOs faces three main challenges: 1) a large number of scattered discharge points, 2) high spatial variation of micropollutant concentrations between sites, and 3) the high temporal variability of flows and concentrations in discharge events. Indeed, especially in dry seasons, the frequency of overflow events of sufficient magnitude for effective sampling may be very low, if not absent. Therefore, the amount of annual sampling campaigns can hardly be increased, with the aim to keep constant the number of samples collected per season.

All samples (1 L) were collected during the first 24 h of a CSO event occurring after a minimum 2-day dry period, where pollutant loads are expected to be higher due to the effect of road and sewer washouts (Masi et al., 2023). Samples covering the overflow hours (for a maximum of 24 h) were collected at the inlet of the VF stage by an automatic sampler, set up to collect composite samples (80 mL every 250 m^3) starting from the beginning of the CSO event. Grab samples were collected for the first VF stage and the second FWS stage outflow. All samples were stored in glass bottles at 4 °C in a dark environment before the laboratory analysis.

For each sample, some physical and chemical parameters, such as conductivity, COD, TSS, $N\text{-}NO_2^-$, $N\text{-}NO_3^-$, and methylene blue active substances (MBAS) were analyzed by an internal certified laboratory, according to standard methods (American Public Health Association, 2005).

2.3. Sample treatment

Given the complexity of the matrix, rich in organic matter and possible interferents that may affect the following spectroscopic analyses, the optimization of the water samples pretreatment for MP analysis represents one of the most significant steps in the procedure.

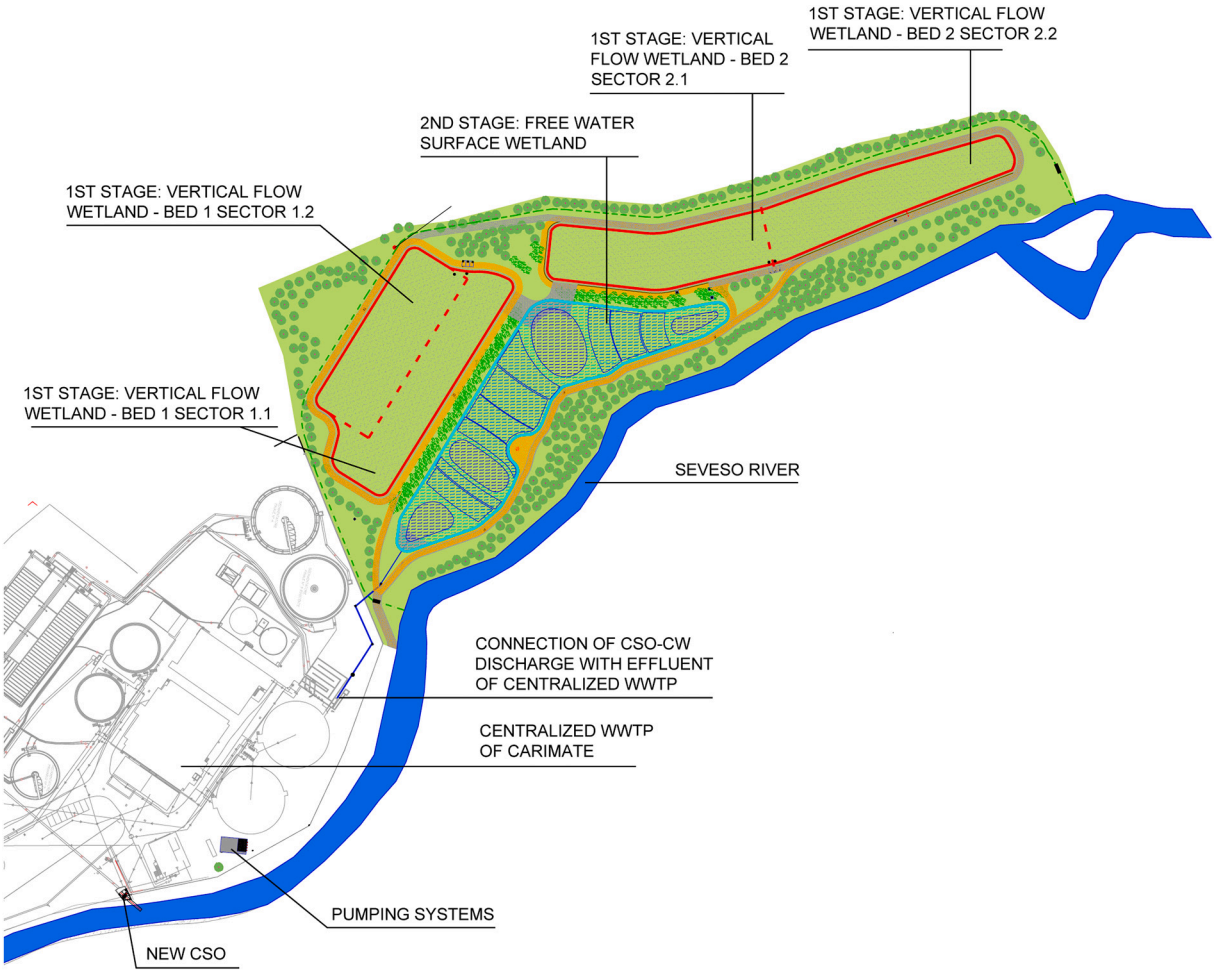

Fig. 1. Layout of the combined sewer overflow-constructed wetland (CSO-CW) system upstream of the wastewater treatment plant (WWTP) in Carimate (Italy). 1st stage: 2 vertical subsurface flow (VF) CW beds (delimited by solid red lines), each bed is divided into 2 hydraulically separated sectors (separated by dashed red lines); 2nd stage: free water surface wetland (FWS) (delimited by solid light blue line) (Masi et al., 2023).

Different digestion conditions and sample volumes were tested to maximize the recovery of MP extraction, avoiding potential polymer damage, and reducing the organic particulate fraction. After optimization, water samples were digested with 30 % hydrogen peroxide at 55 °C for 48 h. Due to the low density of most plastic polymers, the digested samples were separated by density with a saturated sodium chloride solution (1.2 g cm^{-3}) in a separating funnel, in accordance with the method described by Zhou et al. (2022). After 24 h, the supernatant was filtrated through glass microfiber filters (47 mm diameter, GF3 grade, 1.2 μm retention rate, supplied by CHMLAB GROUP) using a glass vacuum filtration apparatus. To ensure that high-density MPs were not missed, the particulate collected at the bottom of the separation funnel was subjected to a secondary identification process according to the protocol of Zhou et al. (2022). In this study, the combination of sample pretreatment and limited sample volume facilitated the separation of high-density MPs from the deposited particulate. For samples with more impurities or larger volumes, a higher-density solution, such as NaI or $ZnCl_2$, should be preferred to keep the high-density plastics in suspension. All filters were placed in clean Petri dishes and stored in a desiccator until subsequent instrumental analysis.

2.4. Sample analysis

2.4.1. Microplastic analysis

All filters were visually examined under a stereomicroscope with an integrated microscopic camera. In accordance with the definition of MP commonly accepted in the literature (Scopetani et al., 2021; Hartmann et al., 2019), only particles smaller than 5 mm were quantified and classified based on their shape, size, and color.

For the chemical characterization of the microparticles (in the range of 10 μm to 5 mm), all dry filters were examined using direct 2D imaging-Fourier transform infrared (FTIR) analysis in reflectance mode, without further sample preparation. The analysis was carried out with a Cary 620–670 FTIR microscope equipped with a Focal Plane Array (FPA) 128 × 128 detector (Agilent Technologies). The spectra and background were recorded in reflectance mode on the surface of the samples (or Au background), using an open aperture and a spectral resolution of 8 cm^{-1}, acquiring 128 scans for each spectrum. Each "single-tile" measurement yields a 700 × 700 μm^2 IR map (128 × 128 pixels) of the sample's surface, where each pixel has dimensions of 5.5 × 5.5 μm^2. In this way, from tens to hundreds of independent IR spectra are collected for each particle (fibers, fragments, etc.), and the detection limit of the FPA detector is in the order of 0.02 pg/μm^2 (Scopetani et al., 2021). The 2D IR maps depicted the intensity of characteristic bands of the investigated polymer, with the chromatic scale indicating increasing absorbance as follows: blue < green < yellow < red (Bartoletti et al., 2020). All the spectra were assigned using standard references from the literature, checking the whole spectral profile of each sample (see Section 3.3). To enhance the reliability of the chemical characterization all detected particles have been characterized. This comprehensive approach, despite being time-consuming, allows for a more precise outcome by reducing the risk of over- or under-estimations, especially given the heterogeneous distribution of MPs on the filters and the abundance of natural fibers that can be easily mistaken for MPs.

2.4.2. Metals and semimetals analysis

For the quantification of metals and semimetals, all the samples were analyzed by inductively coupled plasma atomic emission spectroscopy (ICP-OES) using standard parameters, according to the APAT CNR IRSA 3020 method.

2.5. Quality control

To ensure the reliability and accuracy of MP analysis, a comprehensive quality control protocol has been established. The protocol includes avoiding any plastic material to prevent the potential introduction of extraneous particles. During the sampling phase, field blanks were prepared by placing open Milli-Q water bottles (1 L) next to the sampling points for the duration of the sample collection. These field blanks were then processed following the same protocol used for the samples. Contamination of the laboratory benches was monitored regularly to maintain a clean working environment. Researchers were required to wear lab coats of a known fabric and color to easily identify the potential presence of microfibers from self-contamination and subtract them from sample results. The use of aluminium foil was implemented to prevent atmospheric contamination and photoreactions during the analysis. To further safeguard the integrity of the samples, they were stored under refrigerated conditions. The analysis was conducted in a laminar flow hood to minimize the risk of external contaminants compromising the results.

Control blank samples were tested in triplicate using Milli-Q water (10*L*) to ensure the absence of cross-contamination during the analytical process. Therefore, MP counts in the field samples data were corrected by subtracting the items detected in the black samples. Moreover, possible contamination from the polymeric components of the automatic sampler (e.g. tubes) was accounted for by removing particles of the same color and material from the total amount of detected MPs.

In addition, positive controls were conducted to validate the efficiency of the MP extraction. For the assessment of the recovery, 10 L of water sample were spiked with a known quantity of standard reference material: PE microspheres (particle size 425–500 μm and density 0.96 g cm^{-3}, Cospheric) and PMMA microspheres (particle size 425–500 μm and density 1.20 g cm^{-3}, Cospheric). The tests showed an average recovery of 87 % proving the high efficiency of the analytical procedure.

2.6. Ecological risk assessment

The assessment of MP-associated risk poses significant challenges due to the lack of a standardized approach, including uniform sampling, quantification methods, and well-defined environmental MP concentrations (Haegerbaeumer et al., 2019; Koelmans et al., 2022). In the absence of a specific regulation or a systematic and standardized model for MP ecological risk assessment, recent studies have proposed a modified version of the assessment model applied by Hakanson (1980) for aquatic pollution control. Therefore, in the present study, an ecological risk assessment of MP contamination at different stages of the CSO-CW system of Carimate was conducted based on previous research by Lithner et al. (2011), Xu et al. (2018), Liu et al. (2019b), Li et al. (2020), Pan et al. (2021) and Castillo et al. (2024). A comprehensive assessment of the risks posed by MPs requires considering both their concentration and chemical composition. Following the framework proposed by Lithner et al. (2011), the concept of chemical toxicity associated with MP polymers was then used as a basic index to evaluate the correlated ecological harm. This approach incorporated the hazard scores assigned to plastic polymers and tabulated by Lithner et al. (2011), using the polymer types of detected MPs as key indexes for the risk assessment.

The assessment model for potential ecological risk was calculated as follows:

$$\boldsymbol{E_i} = \boldsymbol{T_i} \times \boldsymbol{CF_i}, \boldsymbol{RI} = \sum_{i=1}^{n} \boldsymbol{E_i}, \boldsymbol{CF_i} = \left(\frac{\boldsymbol{C_i}}{\boldsymbol{C_{0i}}}\right)$$

where E_i and RI are defined as the potential ecological risk factor and potential ecological risk, respectively; T_i is the chemical toxicity coefficient for the constituent polymer (Lithner et al., 2011). The CF_i for MPs is calculated as the ratio of the MP concentration at each sampling point (C_i) to the minimum observed MP concentration (C_{0i}). In the absence of available background data, we adopted the lowest MP concentration measured during our study as a baseline value, in line with the approach proposed by Li et al. (2020).

In addition to E_i and RI values, the hazard scores of plastic polymers

and polymer types were used as indexes for the assessment of MP calculated polymer risk index (Lithner et al., 2011), as follows:

$$H = \sum P_n \times S_n$$

where H is the calculated polymer risk index attributed to MPs, P_n is the percentage of MP polymer types registered at each sampling point for each season, and S_n is the score assigned to the polymer compound constituting the MP particles according to Lithner et al. (2011).

In cases where extensive geographical areas are involved, reliance on a single indicator may prove inadequate. In these scenarios, the pollutant load index (PLI) can be used as an additional dimension of assessment. Indeed, Tomlinson et al. (1980) introduced the PLI as a standardized metric for assessing pollution levels in estuaries, providing a consistent framework for evaluating the contamination grade of different extended regions (Angulo, 1996). Additionally, the method of Tomlinson et al. (1980), originally proposed to assess the status of metal pollution in aquatic environments, has recently been adapted and applied to evaluate the degree of MP contamination in both sediments (Ranjani et al., 2022) and surface water (Pan et al., 2021). The PLI is related to the MP concentration factors (CF_i) and calculated as follows:

$$PLI = \sqrt{CF_i}$$

The criteria for classifying risk levels based on the risk index and the pollution load index are detailed in Table 1, in accordance with the above-described approaches proposed by Liu et al. (2019b), Li et al. (2020), Pan et al. (2021) and Ranjani et al. (2022).

2.7. Data analysis

All data relating to the abundance and classification of MPs were collected and calculated using Microsoft EXCEL 365. Pearson correlation analysis was used to assess the correlation between MPs and physico-chemical indicators. All statistical and data analyses were performed using Origin 2024.

3. Results and discussion

3.1. Microplastic abundance and removal

The number of MPs detected in each sample was normalized by the volume of filtered water, consequently expressing their concentration as items per Liter (items L^{-1}). Only plastic materials have been included in MP concentration, excluding natural polymers, such as cellulose. As shown in Fig. 2 and Table S1, MPs were detected in all the water samples with a range between 25 ± 5 and 300 ± 57 items L^{-1}. Generally, the results revealed a remarkable pattern in MP concentrations. A reduction of MPs was indeed observed passing from inlet to outlet samples of the first vertical flow stage, indicating a significant removal efficiency in this section of the treatment process. Interestingly, however, MP levels partially increased after the second FWS stage.

Additionally, a significant trend can be observed with a gradual increase in MP concentrations during the wet season. Consistent with both identified patterns, the lowest recorded concentration, amounting to 25 ± 5 items L^{-1}, was documented during the summer sampling campaign for VF stage outlet samples, while the highest concentration, totaling 300 ± 57 items L^{-1}, was recorded for winter water samples collected at the inlet of Carimate CSO-CW system.

Table 1
Risk assessment of MPs pollution and relative categories.

Risk category	Minor	Medium	High	Danger	Extreme danger
E_i	<40	40–80	80–160	160–320	>320
RI	<150	150–300	300–600	600–1200	>1200
H	0–1	1–10	10–100	100–1000	>1000
PLI	<10		10–20	20–30	>30
Hazard level	I	II	III	IV	V

Generally, MP research faces significant challenges due to the lack of standardization of sampling methodologies, use of various analytical techniques (i.e. pyrolysis-gas chromatography–mass spectrometry (Pyr-GC/MS), Raman/micro-Raman spectroscopy, and infrared (IR) spectroscopy) and, consequently, units of measurement (Rathore et al., 2023). While recognizing the intrinsic difficulty of comparing data obtained following different analytical protocols, the results of this study are generally consistent with those reported in the literature regarding the association between MPs and CSO events (Table 2). A final consideration regarding MP abundance levels concerns the significant fluctuations that may occur, especially when studying stochastic and variable events such as CSOs. Therefore, it is important to note that the data discussed in this study represent a picture of the four seasonal sampling campaigns under investigation. Further research and an increased number of samples, although challenging due to the intrinsic nature of CSOs as discussed in Section 2.2, may reveal additional variability in MP concentrations.

The level of mitigation performance achieved at the different stages of the CSO-CW system for each season is presented in Fig. 2. MP removal efficiency obtained after the first VF stage and the second FWS stage were respectively: 40 %, 20 % in spring; 77 %, 59 % in summer; 71 %, 43 % in autumn; 67 %, 40 % in winter. Despite seasonal variations, the MP removal rate demonstrated by VF CW is significant and generally in line with what has been reported in previous studies for other full-scale systems (Table 3). However, a lower-than-average removal rate was recorded in spring due to a possible correlation between the smaller number of particles determined in the volume unit and the mitigation capacity of the CW system. Previous studies have already shed light on the relatively lower MP removal efficiency associated with FWS-CW systems compared to alternative configurations, such as VF CW (Chen et al., 2021; Xu et al., 2022). These results are further confirmed by Wang et al. (2021), who clarified that when using exclusively FWS-CW systems, MP removal rates decrease significantly. A similar picture is underlined by the research conducted by Chen et al. (2021), who advanced the idea that physical filtration emerges as the main mechanism by which CWs remove micro and nanoplastics from wastewater.

Despite these considerations, the partial increase in MP levels after the second FWS was unexpected. A possible explanation for these results may be found both in the stochasticity of CSO events and in the different hydraulic characteristics of the VF and FWS systems. In fact, CSOs are generally characterized by a non-uniform level of contamination over time. In addition, the treated water is rapidly filtered by the VF CW stage with an expected low level of sedimentation and a short average retention time of about 3/4 h. Therefore, grab samples may show highly variable levels of MP contamination depending on the time of collection. In contrast, the FWS stage is characterized by a considerably longer retention time (up to 48 h) and therefore provides a more comprehensive view of the overall effectiveness of the multi-stage CW treatment throughout the overflow event. Another relevant aspect is that in the absence of CSO events, the FWS stage is not fed and the resulting evaporation of water within the system can lead to a concentration of MPs associated with previous overflows. During the following CSO, the increased flow causes a significant flushing of sediments at the bottom of the system, resulting in a potential increase in MPs detected in FWS outlet samples. In this instance, a different model should be applied to calculate the removal efficiency of the FWS system. A possible improvement of the calculation could include the addition of a correction factor to account for the amount of MPs accumulated due to previous dry seasons. However, further investigations are essential to gain a deeper understanding of MP removal and accumulation in CWs with different designs. To address these knowledge gap, it would be beneficial to collect targeted 24-h composite samples. In addition, future perspectives include the construction of specific pollutograms which, by plotting the abundance of contaminants against the time and water

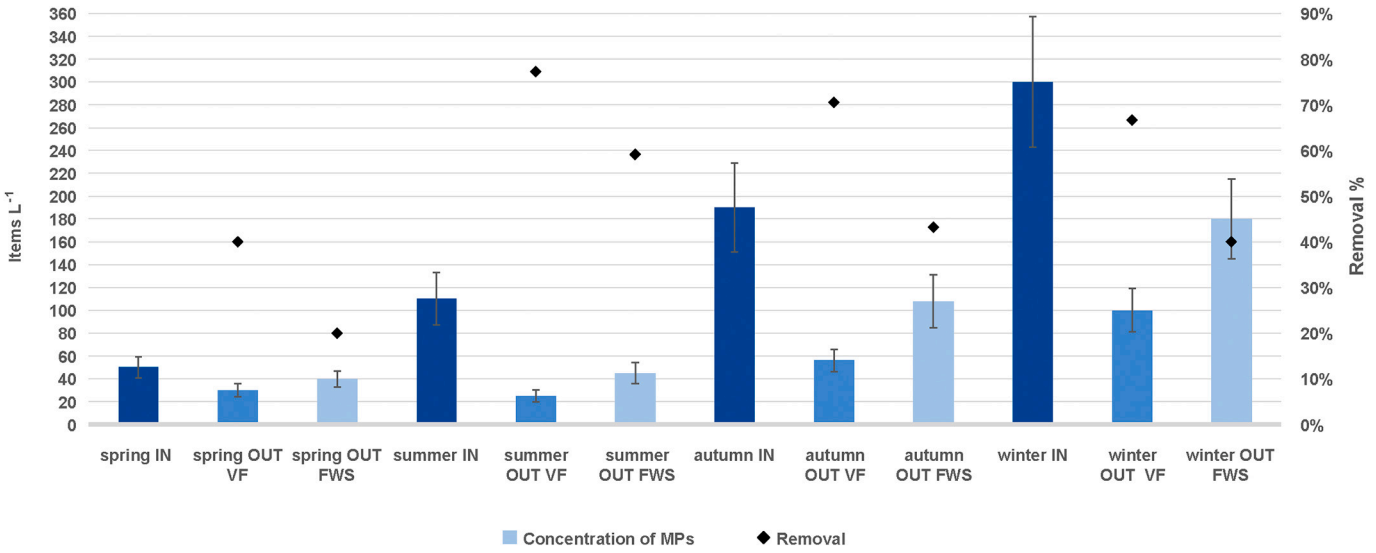

Fig. 2. Seasonal variation of mean MP abundance (histograms) and MP removal efficiency (black diamonds) at different stages of Carimate CSO-CW system: IN (inlet of the CSO-CW system) in dark blue, OUT VF (outlet of the first vertical flow stage) in blue, OUT FWS (outlet of the second free water surface stage) in light blue. The samples were collected during four different seasonal sampling campaigns in 2022.

Table 2
Current study on the abundance of microplastics discharged by combined sewer overflows.

Region	Abundance of MPs	Size range	Sampling method	Analysis method	Reference
Italy	163 ± 32 items L^{-1} [a]	10 μm- 5 mm	Automatic sampler (inlet) and grab samples (outlet)	Stereomicroscope and Micro-FTIR	Present study
France	190–1046 fibers L^{-1} 35–658 fragments L^{-1}	100–5000 μm	Automatic sampler	Stereomicroscope	Dris et al., 2015
Baltic Sea catchment	59,000 Items yr^{-1} or 2.1 ton yr^{-1} (median)	10 μm- 5 mm	Not available (data extracted from publicly accessible databases)	Not available (data extracted from publicly accessible databases)	Baresel and Olshammar, 2019
	125 ng L^{-1} (estimated concentration calculated with a model)	Not available	Not available	Stereomicroscope and micro-FTIR	Bollmann et al., 2019
China	83.1 ± 40.2 items L^{-1}	30 μm- 5 mm	10 L stainless-steel bucket	Stereomicroscope and micro-FTIR	Zhou et al., 2023
	8500.0 ± 1241.0 items L^{-1}	40 μm- 5 mm	Automatic sampler	Stereomicroscope and micro-FTIR	Sun et al., 2023
Hudson River Park (New York)	198,000 particles km^{-2} (median)	333 μm- 5 mm	Samples were collected using a 333 μm mesh, 1 m wide, 3 m long Neuston net with a 1 L plastic bottle attachment	Stereomicroscope	Polanco et al., 2020

[a] Mean concentration for inlet samples.

volume during rainfall events, can provide a more detailed assessment of potential peak of MP concentrations and their removal dynamics in different CW types within overflow events.

As a final consideration, although research on MP migration and accumulation within CWs remains limited, physical interception involving plant roots, substrates, and biofilms has been identified as the main mechanism for MP removal in CWs (Liu et al., 2023). Given the predominance of filtration as the primary MP remediation process (Chen et al., 2021), it would be beneficial to investigate the correlation between MP removal performances and the type of filter medium used in the CW system. As illustrated in Table 3, most of the available research have focused on CWs filled with gravel. It would be interesting to investigate and compare the mitigation efficiency of sand-based systems, such as unsaturated VF CWs design according to the German approach for municipal water treatment and Retention Soil Filters (RSF) for CSO treatment (Tondera, 2019; Rizzo et al., 2020), which may potentially better retain MPs due to a smaller particle size of the media. Therefore, the substrate composition of CWs certainly plays a key role in the filtration, adsorption, and retention processes involved in MP removal (Liu et al., 2023). Wang et al. (2020) conducted an evaluation of HSF-CWs for the removal of MPs from wastewater. The authors highlighted the close relationship between the diameter and porosity of the substrate and MP removal. As expected, substrates with lower porosity demonstrated more effective MP removal capacities due to more efficient retention of the particles. In accordance, Lu et al. (2022) highlighted the efficacy of sediment in trapping MPs within CWs, emphasizing that the number of MPs recorded in the media increased as the grain size of the substrate decreased. In addition, enhancing the mineral content of wetland substrates has been shown to improve MP removal, as observed by Qian et al. (2021). Indeed, increased mineral content leads to improved MP trapping and retention, with metal cations playing a positive role in this process. Similarly, aluminosilicate filter media have been found effective in MP removal, particularly when modified with cationic surfactants, achieving a retention capacity >96 % due to direct binding between negatively charged MPs and minerals (Shen et al., 2021). Moreover, to delineate a complete picture of the long-term fate of filtered MPs, it is essential to collect a significant amount of evidence on all pathways that MPs may undergo within CW systems, including adsorption, biological degradation, and potential plant uptake.

Table 3
Current study on removal of microplastics by full-scale constructed wetlands. FWS-CW: free water surface flow constructed wetland, SSF-CW: subsurface flow constructed wetland, HSF-CW: horizontal subsurface flow constructed wetland, and VF-CW: vertical subsurface flow constructed wetland.

Region	Water treated	Design parameters			Microplastics characteristics			Removal rate	Reference
		Structural types	Plant species	Substrate	Polymer	Size (μm)	Shape		
UK	Secondary municipal WWTP effluent	FWS-CW	*Schoenoplectus lacustris and Typha angustifolia*	Gravel	–	>1000 (large), 100–1000 (medium) and < 100 (small)	Fibers and fragments	95 %	Bydalek et al., 2023
China	WWTP effluent	HSF-CW + SSF-CW	*Reed, Gattail, Scallion*	Gravel (d 60–90 + 20–50)	PP, PS, PET, PES, and PE, PA	–	Fibers, films, fragments, others	85.8–93.7 %	Zhou et al., 2022
	Rural domestic wastewater	SSF-CW	*Canna and calamus*	Gravel (d 60–90 + 20–50 mm) Gravel (d 5–40/ 30 % + 40–80/40 %)	PP, PS, PET, PES, and PE, PA	–	Fibers, fragments, others	45–100 %	Wei et al., 2020
Belgium	Secondary WWTP effluent	HSF-CW	*Reed*	System 1: Coarse gravel (d 60–90 mm); medium and fine gravel (d 20–50 mm) System 2: medium and fine gravel (d 20–50 mm) Coarse gravel (d 30 ~ −50 mm); medium and fine gravel (d 5–30 mm)	–	75–425	Fiber, grain	88 %	Wang et al., 2020a
Australia	Stormwater and wastewater	stormwater CW	–	Sediment	PE, PET, PP, and others	25–5000	Fibers, fragments	82 %	Lu et al., 2022
–	–	VF-CW+ SSF + CW	*Reed, Cattail*	Gravel (d 5–50 mm)	PET, PE, PS, PP, and PVC	–	Fibers, particles, fragments, and films	30–76.5 %	Xu et al., 2022
–	–	FWS-CW	*Reed, Cattail, Scallion*	Coarse gravel (d 60–90 mm); medium and fine gravel (d 20–50 mm)	–	–	–	29.4 ± 1.4 %	Xu et al., 2022
Italy	Combined sewer overflow	VF-CW+ FWS-CW	*Phragmites australis + Schenoplectus Lacustris, Menyanthes Trifollata, Typha minima, Nimphea Alba, Lythrum Salicaria, Nuphar Iutea, Iris Pseudacorus, Carex riparia, Typha latifolia, and Pesicria Amphibia*	coarse gravel (d 20–40 mm); gravel (d 5–10 mm); pea gravel (d 1–5 mm	PET, PS, PAN, ABS, PP/PE, cellulose	20–4000	Fibers and fragments	20–77 %	Present study

3.2. Physical characterization of microplastics

Factors such as size, shape, density, and color can significantly influence the environmental distribution and toxic effects of MPs (Singh et al., 2021). For instance, the shape of the particles can facilitate traceability and influence adsorption and ecological impacts (Ahmed et al., 2024). In this study, two different shapes only, fibers and fragments, were detected in all filters analyzed. As shown in Fig. 3a, all the sampling sites for each season were dominated by fibrous MPs with a percentage ranging from 61 %, detected for inlet water samples collected in autumn, to 99 %, recorded for VF outlet in spring. The average percentage recorded for fibers versus fragments was 76 %.

Size plays a crucial role in both the MP impact on ecosystems and the filtration retention performance of different media (Rose and Webber, 2019). In general, smaller particles exhibit larger specific surface areas, enhancing the absorption of chemicals and microorganisms, and potentially amplifying global toxicity (Lu et al., 2022). Therefore, in the present study, particles smaller than 5 mm were divided into 5 dimensional subcategories. Data show a general prevalence of items in the range of 100 to 499 μm, with a peak of 67 % recorded for spring OUT VF samples (Fig. 3b). Although the detection of a specific trend is challenging, it is possible to observe that the proportion of small particles (<100 μm and 100–499 μm) gradually increases in the outlet samples, if compared to inlet water samples collected in the same period. Simultaneously, MPs of larger sizes (2–5 mm) decrease significantly, reducing from a mean of 15 % in the inlet samples to 1 % and 4 % in the VF OUT and FWS OUT samples, respectively. This pattern indicates that larger particles are more efficiently removed by both the first vertical flow stage and the second FWS polishing treatment. A better retention rate for MPs above 500 μm is consistent with the size distribution profile described for other constructed wetland systems in the literature (Lu et al., 2022).

Regarding color classification, which can support the identification of contamination sources and assess the polymer degradation levels (Ahmed et al., 2024), a significant variability characterizes the MPs of each sample without a definite seasonal trend (Fig. 3c). In general, the most abundant detected colors were blue and black. A consideration can be made about transparent particles, mostly fibers, which accounted for

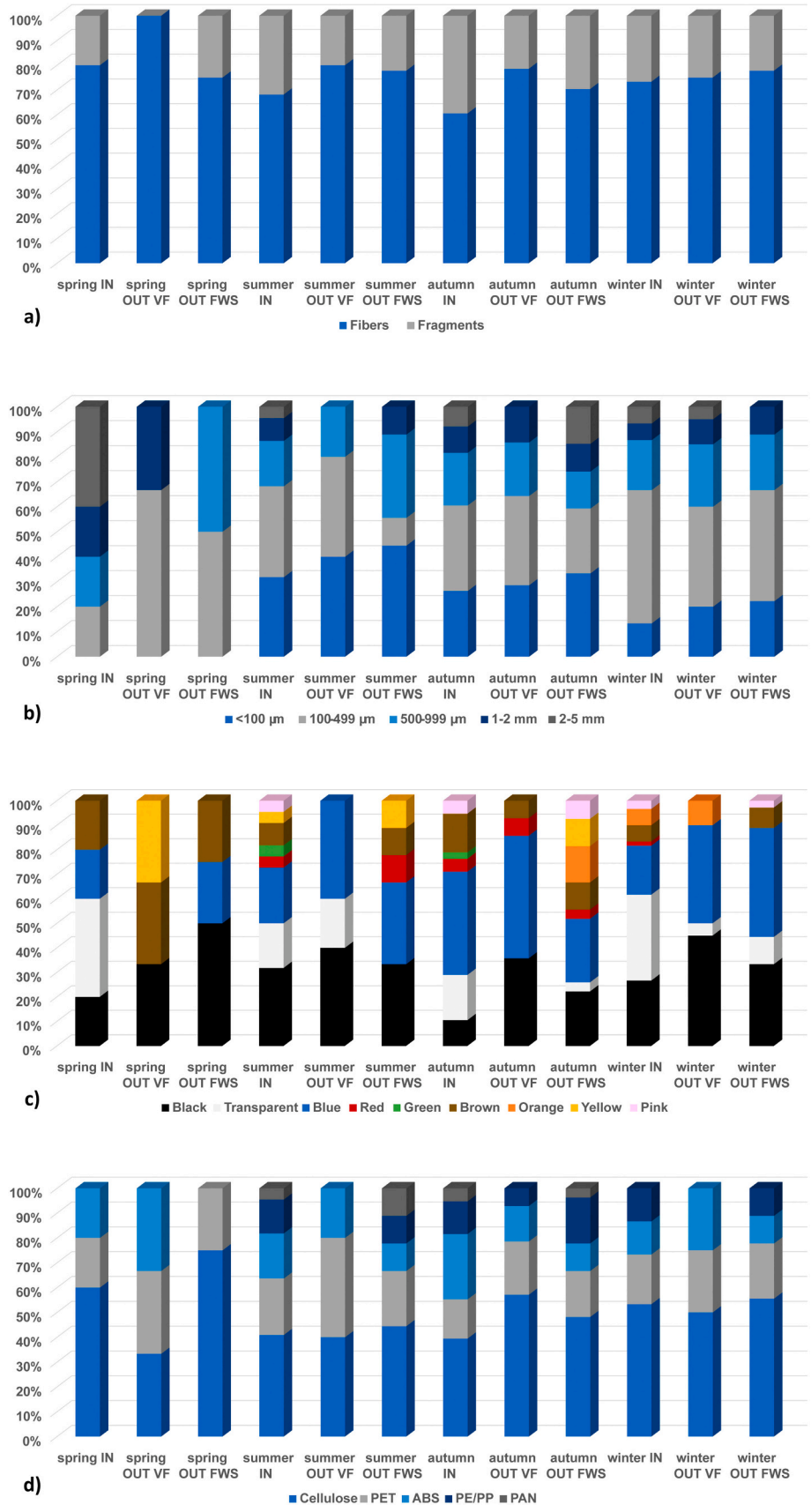

Fig. 3. Seasonal variation of percentage of MP characteristics for the three sampling points: IN (inlet of the CSO-CW system), OUT VF (outlet of the first vertical flow stage), OUT FWS (outlet of the second free water surface stage). The samples were collected during four different seasonal sampling campaigns in 2022. Classification of MPs detected in the water sample based on different shape (a), size (b), color (c), and chemical characterization (d).

an average of 28 % for inlet samples and decreased to 6 % and 4 % for VF OUT and FWS OUT samples, respectively. The decrease of transparent particles percentage combined with the increasing rate of dark particles (blue and black) in all outlet samples suggest that, during the two stages of treatment, the Nature-Based Solution (NBS) system does not stimulate the release of pigments and dyes from the plastics to the water, a factor that could pose an additional risk to the ecosystems of receiving water bodies.

3.3. Chemical characterization of microplastics

Polypropylene (PP), polyethylene (PE), polyethylene terephthalate (PET), polystyrene (PS), polyacrylonitrile (PAN), acrylonitrile butadiene styrene (ABS), and cellulose were identified by FT-IR spectroscopy (Fig. 3d). The relative mean abundance of each type of micro-items was as follows: cellulose (50 %), PET (24 %), ABS (17 %), PE/PP (7 %), and PAN (2 %).

The detection of these polymers is predictable as they represent some of the most widely manufactured and commonly used plastic products and are consistent with available literature studies. For instance, Wei et al. (2023) report that PP, PE, and PET represent >80 % of all polymers in rainwater/stormwater environments. Similar data were presented in the review by Wang et al. (2022) on the global occurrence and characteristics of MPs in urban runoff.

Although they do not represent a plastic material, cellulose fibers were included in the reported results of the chemical characterization analysis to emphasize the importance of a comprehensive characterization of all detected particles to avoid overestimation of plastic polymers similar in buoyancy, shape, and color. Additionally, the detection of cellulose microfibers can potentially signal two primary sources of pollution. Firstly, cellulose fibers may originate from natural and synthetic fabrics, including cotton and Rayon. Secondly, they could originate from cigarette filters, which are composed primarily of Rayon (Scopetani et al., 2021) and represent a significant source of contamination in heavily anthropized urban areas. Although it is important to note that Rayon and cellulose fibers themselves do not pose a significant environmental risk, they can bind and subsequently release potentially hazardous additives such as phthalates and dyes, which could represent an environmental and biota-associated threat (Zambrano et al., 2021). This concern is further heightened when considering the substantial number of cellulose-based fibers identified in our water samples (mean concentration: 51 fibers L^{-1} and 120 fibers L^{-1}, in the effluent of the VF and FWS, respectively). Furthermore, the presence of PAN and PET fibers, which are used in textile production in addition to cellulose fibers, supports the hypothesis that one of the primary domestic sources of MP pollution is represented by washing machines. In line with the dual nature of the source that constitutes CSOs, PET may additionally derive from the urban runoff. Indeed, this polymer is widely used in urban environments (Wei et al., 2023), with a broad range of applications, including automotive textiles. For a complete understanding, Fig. S2 shows the average percentage of each plastic polymer, excluding non-plastic materials such as cellulose.

Regarding micro-fragments, the predominant composition observed in all water samples comprises nearly exclusively ABS, with a smaller proportion of PE and PP. PE and PP were combined into a single subcategory in our analysis, mainly due to the frequent detection of blends of the two polymers. The presence of PP and PE in rainwater/stormwater from urban areas has already been identified and is mainly attributed to the improper disposal and degradation of everyday products such as single-use plastic bags, food containers, and packaging materials (Wei et al., 2023). Of particular interest is the blue coloration of most the ABS fragments, consistent with this polymer's widespread use in pipe components. This raises questions about the potential points of MP release, particularly within the sewer drainage system itself. It is plausible that the wastewater stream came into contact with the ABS material during its transit through sewage drains. This contact could have led to the partial fragmentation of the ABS, introducing an additional source of contamination. Furthermore, the presence of ABS in the inlet samples effectively dismisses the possibility that this contamination could have been introduced within the confines of the CSO-CW system. Further investigation into the specific sources and pathways of this class of MPs into the aquatic environment is warranted to gain a full understanding of their environmental distribution and impact.

Fig. 4a shows a blue fiber characterized by spectra showing bands indicative of PET at about 3000–2800 cm^{-1} corresponding to aromatic and aliphatic CH stretching, a notable band at 1730 cm^{-1} representing C═O stretching, as well as distinct peaks at 1580 and 1504 cm^{-1} indicating aromatic C═C stretching. In addition, the spectrum shows a distinguishable peak at 1412 cm^{-1} associated with aromatic skeletal stretching and another at 1235 cm^{-1}, characteristic of C—O stretching (Chen et al., 2012; Jung et al., 2018; Pereira et al., 2009). The peak at 3430 cm^{-1} can be attributed to an overtone of the C═O.

Fig. 4b presents a fiber identifiable as PAN owing to the presence of bands in the 3000–2800 cm^{-1} region, associated with C—H stretching, at 2237 cm^{-1} (C≡N stretching), 1740 cm^{-1} (C═O stretching), 1440 cm^{-1} (δas CH_2), and 1365 cm^{-1} (δs CH_3) (Coates, 2006; Jung et al., 2018). The sharp and intense carbonyl stretching band at 1735 cm^{-1} suggests the presence of an acrylate polymer rather than an oxidation band, which is typically weaker and broader (Gardette et al., 2013). This observation is not surprising as one of the most widely adopted acrylic fibers is derived from the copolymerization of acrylonitrile with vinyl acetate.

Fig. 4c shows a blue fragment, identified as ABS due to the characteristic absorptions at 3023 cm^{-1} (C—H aromatic stretching), in the 3000–2800 cm^{-1} region (C—H stretching), at 1602 cm^{-1} (aromatic ring vibration), at 1494 cm^{-1} (aromatic ring vibration) and 1454 cm^{-1} (CH_2 bending) (Jung et al., 2018). In this case, the absorption at 1730 cm^{-1} was attributed to a subsequent oxidation of the polymer. The three peaks above 3500 cm^{-1}, on the other hand, are diagnostic of the presence of silicates deposited on the surface of the fragment (Saikia and Parthasarathy, 2010).

3.4. Association between microplastics and environmental factors

Based on the results of the Pearson correlation analysis, the relationship between different water quality and quantity parameters and MP concentrations in inlet water samples was evaluated ($p < 0.05$).

Regarding the water quantity factor, the correlation between MP concentrations and the flow rate (expressed in m^3d^{-1}) treated by the Carimate CSO-CW system provides interesting results. In fact, the flow rate can be considered as a translation of the corresponding storm intensity, since the multistage CW system is only activated during overflow events that occur upstream of the centralized WWTP. As shown in Fig. 5a and b, the volume of water treated per day has a significant impact on the MP abundance of CSOs during wet weather. Consistent with the findings of Sun et al. (2023), MP concentrations increase with the intensity of rainfall events. Considering that all samples in this study were collected during the first 24 h of CSOs, the correlation between these two parameters may be the result of the 'first flush' phenomenon, which has been shown to be responsible for higher levels of pollutants in the early stages of a storm event (Mamun et al., 2020). This effect becomes more pronounced as the number of previous dry days and storm intensity increase (Luo et al., 2009). Further evidence for this hypothesis is provided by the correlation values between MP concentration and TSS. Indeed, in line with the findings of Sun et al. (2023), the abundance of MPs is strongly correlated with both flow intensity and TSS (Fig. 5.), suggesting a higher release of MPs during the first flush of the CSO event. Furthermore, although further investigation is required, these strong correlations indicate that regularly monitored parameters, such as TSS and flow rate, could help to predict MP peak loads during stochastic CSO events. This finding underscores the potential of using readily available data to enhance pollution prediction and mitigation strategies in urban

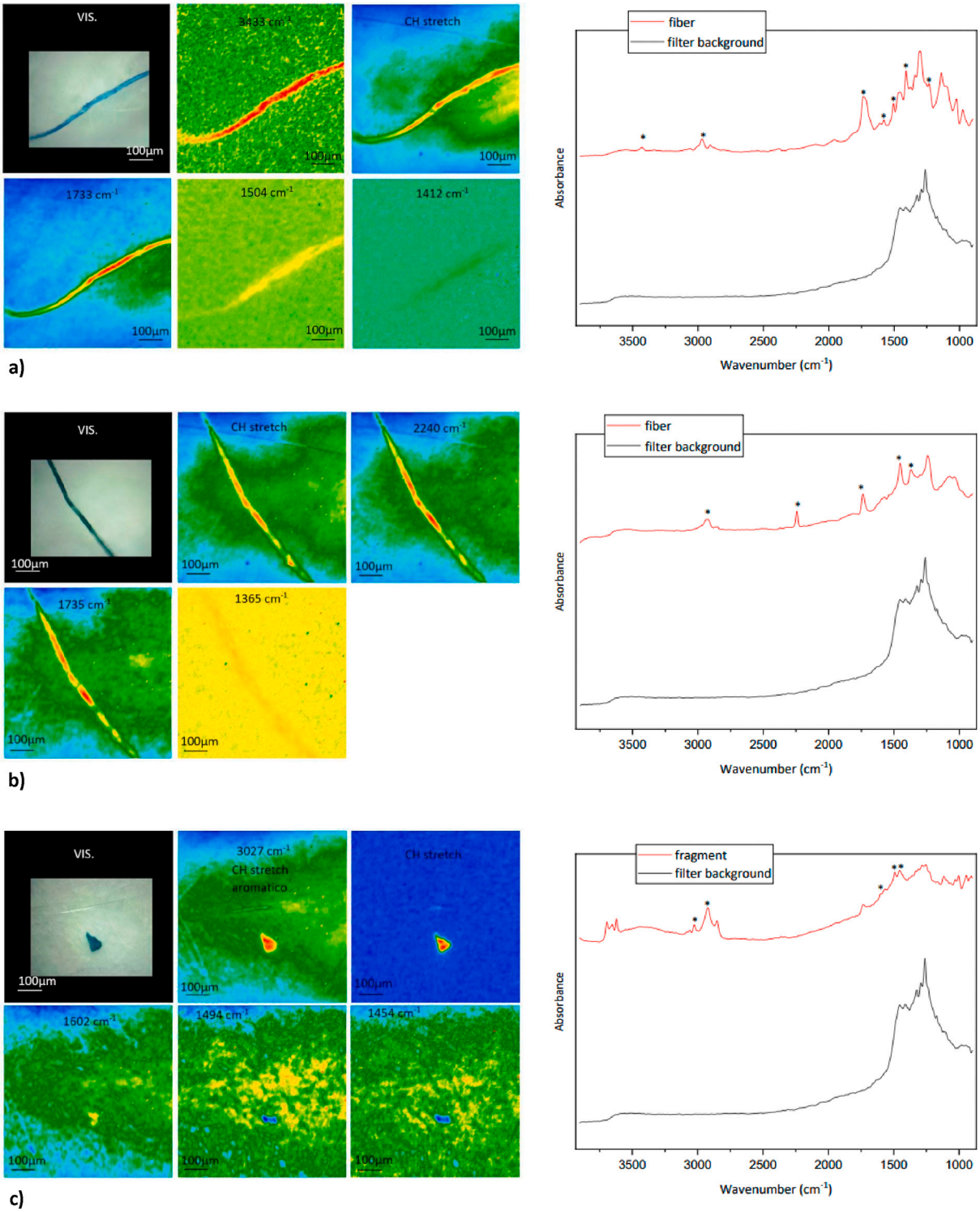

Fig. 4. (a) Blue fiber identified as PET: Visible light map of the filter substrate, 2D FTIR Imaging maps*, and FTIR Reflectance spectrum of the microfiber**. (b) Black fiber identified as PAN: Visible light map of the filter substrate, 2D FTIR Imaging maps*, and FTIR Reflectance spectrum of the microfiber**. (c) Blue fragment identified as ABS: Visible light map of the filter substrate, 2D FTIR Imaging maps*, and FTIR Reflectance spectrum of the microfiber**.
*The chromatic scale of each map qualitatively shows the absorbance intensity as follows: blue < green < yellow < red. Maps have dimensions of 700 × 700 µm^2.
**The spectrum relates to a single pixel (5.5 × 5.5 µm^2) of the 2D Imaging maps, representative of the fiber/fragment absorptions.

water systems.

A positive correlation value was also observed between the level of MP contamination and the quantity of MBAS, which represents an index of the presence of anionic surfactants (such as detergents or foaming agents) in the analyzed water. Future research could deepen our understanding of the mechanisms that determine the correlation between these parameters during CSO events. Exploring how various environmental factors influence these relationships would provide insights into the development of more accurate predictive models of MP pollution in urban water systems.

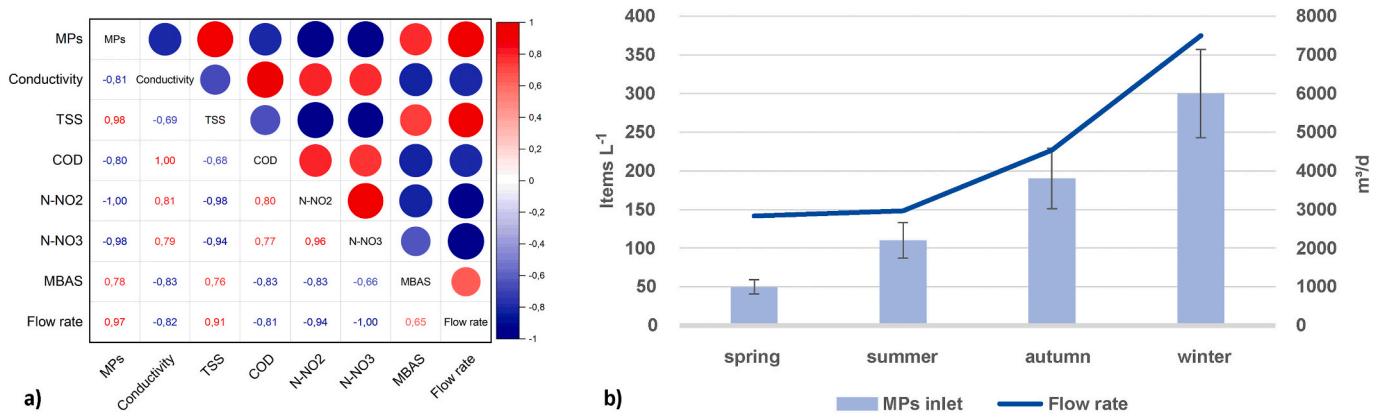

Fig. 5. (a) Correlations between MP concentrations (items L^{-1}) and environmental factors in CSO samples (inlet water samples). (b) Comparison between MP concentration (items L^{-1}) in inlet water samples and flow rate of CSO-CW system.

A second Pearson's test was conducted to assess the potential associations between MP abundance (items L^{-1}) and the concentrations of various metal/semimetal elements in both inlet and final effluent water samples (Fig. 6.). Although none of the elements demonstrated a statistically significant impact on MP occurrence ($p < 0.05$), certain positive correlations were observed. For instance, Ba exhibited strong correlations with Cu, Hg, Mn, Ni, and Se, while Cu showed strong correlations with Mn, Ni, and Se. Additionally, notable correlations were identified between Fe and P, S, and Si, as well as between Ni and P and Se, and among P and S and Si. More details on the seasonal abundance of metals and semimetals are shown in Fig. S3 and S4.

The absence of a positive correlation between MP and metal concentration found in this study is an interesting parameter for a more complete assessment of the threat posed by MPs to the receiving waterbody. MPs indeed possess physicochemical characteristics, such as small particle size, large specific surface area, and hydrophobic nature, that enable them to adsorb various harmful pollutants, including heavy metals (Kutralam-Muniasamy et al., 2021). This adsorption process is facilitated by the presence of functional groups on the surface of MPs, such as hydroxyl and carboxyl groups, which can form complexes with heavy metal ions. Moreover, during the manufacturing process, plastics may inherit metals and organometallic compounds, commonly added to improve polymers' properties and costs (Ashton et al., 2010; Massos and Turner, 2017). Indeed, many additives used in the plastic industry contain heavy metals such as Pb, Cr, Sn, and Ba (Zha et al., 2022). Once adsorbed onto MPs, these elements can be transported over long distances, and potentially released into aquatic ecosystems. Initial reports on heavy metal content in MPs emerged around the early 2010s, with studies investigating the association between plastic pellets production and metals in marine environments (Ashton et al., 2010). Subsequent research has further examined heavy metal occurrence in MPs collected from aquatic ecosystems worldwide, revealing variable levels of concentration and associated environmental toxicity (Patterson et al., 2020; Ta and Babel, 2020). Although these findings have raised increasing concerns about the potential for MP-mediated metal transport to aquatic environments, our study did not demonstrate a direct link between the two parameters for the system under investigation. This result indicates that Carimate CSO-CW does not stimulate the release of metals under these conditions. Further research and comparison with other large-scale CW data are required to assess how systems can be designed to promote the non-release of metals from MPs.

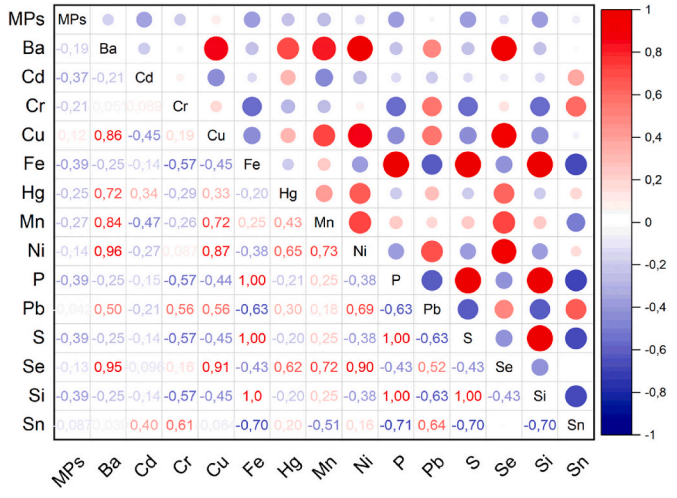

Fig. 6. Correlations between MP abundance (items L^{-1}) and the concentrations of several metal/semimetal elements in CSOs.

3.5. Risk assessment of microplastics

Currently, there is a lack of systematic and standardized models to comprehensively assess the ecological risks posed by MPs. In this research, different indexes, including E_i (Ecological Risk Index), RI (Risk Index), H (Hazard Score), and PLI (Pollution Load Index), were used to investigate the ecological risks associated with MPs released during CSO events. These indexes were specifically applied to evaluate the risk classification of water samples at different treatment stages within the full-scale CSO-CW system upstream of the Carimate WWTP, as shown in Table 4 and illustrated in Fig. 7. and Fig. S5.

Essentially, the ecological risks posed by ABS strongly exceeded those associated with other types of polymers, as evidenced by the elevated E_i values attributed to ABS, mainly due to its significantly higher hazard score (6552) compared to PET (4), PP (1), PE (11) and PAN (10.599) (Lithner et al., 2011). As a result of the presence of ABS fragments in almost all the water samples, the calculated RI values were significantly elevated, placing them in the highest risk category. Nevertheless, the field of MP risk assessment still faces ongoing challenges, including the lack of consistent quantification models and well-defined background levels. Furthermore, MPs can act as vector for a wide range of contaminants, including heavy metals and persistent organic pollutants (POPs) (Zhang et al., 2019; Brennecke et al., 2016), thereby enhancing their intrinsic toxicity. The assessment of this complex interaction between MPs and other pollutants remains an unresolved issue and warrants further investigation.

In this study, the calculated Polymer Risk Index (H) values for the MPs detected at all sampling points during each season were consistently >1000 or in the range from 100 to 1000, indicating the presence of a significant high chemical risk (Table 1). In contrast, the PLI values for all the samples were consistently classified as risk category I, as the

Table 4
Seasonal variations of potential ecological risk (E_i) with colorimetric representation of relative risk category [a]. IN (inlet of the CSO-CW system), OUT VF (outlet of the first vertical flow stage), OUT FWS (outlet of the second free water surface stage).

		E_i			
		PET	ABS	PP/PE	PAN
Spring	IN	11	6552	0	0
	OUT VF	11	6552	0	0
	OUT FWS	11	0	0	0
Summer	IN	28	13104	9	5
	OUT VF	11	3276	0	0
	OUT FWS	11	3276	3	5
Autumn	IN	33	32760	15	11
	OUT VF	13	5242	2	0
	OUT FWS	22	7862	12	4
Winter	IN	66	26208	24	0
	OUT VF	28	16380	0	0
	OUT FWS	44	13104	12	0

[a]

Minor	Medium	High	Danger	Extreme danger

formula does not consider the specific toxicity of the polymers, but only their relative abundance. Overall, as expected, the seasonal variation of potential ecological risk factor (E_i), potential ecological risk (RI), and pollution load index (PLI) mirrored the trends observed for MP abundance, showing an increase with more intense rainfall events in comparison to dry seasons. This multi-faceted approach highlights the need to consider both concentration and chemical composition when assessing the risks associated with MPs, providing a robust and holistic framework for addressing the potential ecological impacts of MP contamination of surface waters.

In summary, although the multi-stage CW system has been shown to effectively remove a significant percentage of MPs present in the inlet samples, the risk analysis indicates that these removal rates are still not sufficient to consider the MPs released into the environment as non-hazardous, mainly due to the non-negligible presence of ABS.

4. Conclusions

This study provides an innovative investigation of MP occurrence and dynamics within CSOs, evaluating the potential of CW systems with different designs for CSO-associate MP mitigation. To the best of our knowledge, this research, which involves the multi-stage CW system of Carimate (Italy), represents the first study on MP removal performance of a large-scale system designed to treat CSO upstream of a centralized WWTP.

The results confirm the significant contribution of CSOs to MP contamination of the receiving water body (maximum inlet concentration: 300 ± 57 items L^{-1}), highlighting a clear increase in MP abundance during intense rainfall events. The strong correlation between MP concentration, flow rate, and TSS values, validates the hypothesis of the first flush phenomenon and its impact on MP release during CSO events. Removal data indicate different MP dynamics depending on the design of the CW units and the predominance of filtration as a key retention mechanism. The first VF stage showed removal rates ranging from 40 % to 77 %. However, the unexpected increase in MP concentrations after

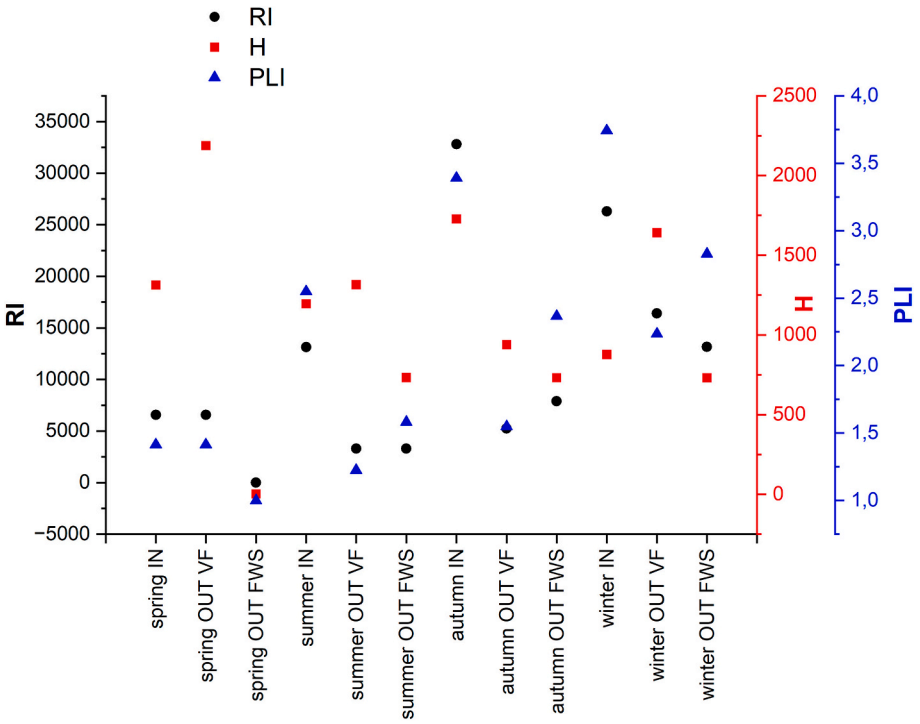

Fig. 7. Seasonal variations of potential ecological risk (RI), calculated polymer risk index (H), and pollution load index (PLI) linked to MP contamination at three different stages of the CSO-CW system of Carimate: IN (inlet of the CSO-CW system), OUT VF (outlet of the first vertical flow stage), OUT FWS (outlet of the second free water surface stage).

the FWS stage suggests the stochasticity of CSO events and the different hydraulic characteristics of the VF and FWS systems have diverse impacts on MP release. The risk assessment analysis highlighted the elevated ecological risks associated particularly with ABS particles, detected in most of the samples. Further efforts are needed to control MP discharges from CSOs and to understand the potential of NBS as MP mitigation strategy.

CRediT authorship contribution statement

Chiara Sarti: Writing – original draft, Methodology, Investigation, Conceptualization. **Alessandra Cincinelli:** Writing – review & editing, Validation, Supervision. **Riccardo Bresciani:** Writing – review & editing, Data curation. **Anacleto Rizzo:** Writing – review & editing, Software, Data curation. **David Chelazzi:** Writing – review & editing, Resources, Investigation. **Fabio Masi:** Supervision, Conceptualization.

Declaration of competing interest

The authors declare that they have no known competing financial interests or personal relationships that could have appeared to influence the work reported in this paper.

Data availability

Data will be made available on request.

Acknowledgements

We acknowledge the Water Utility COMO ACQUA Srl for the sharing of the data used in this publication.

C.S. gratefully acknowledges MUR and EU-FSE for financial support of the PhD fellowship PON Research and Innovation 2014-2020 (D.M 1061/2021) XXXVII Cycle in Chemical Sciences: “Green deal and Zero Pollution strategy: innovative solutions for emerging contaminants removal”.

A.C. and D.C. gratefully acknowledge Consorzio Interuniversitario per lo Sviluppo dei Sistemi a Grande Interfase (CSGI, Center for Colloid and Surface Science) for financial support.

Appendix A. Supplementary data

Supplementary data to this article can be found online at https://doi.org/10.1016/j.scitotenv.2024.175864.

References

Ahmed, S.F., Islam, N., Tasannum, N., Mehjabin, A., Momtahin, A., Chowdhury, A.A., Almomani, F., Mofijur, M., 2024. Microplastic removal and management strategies for wastewater treatment plants. Chemosphere 347, 140648. https://doi.org/10.1016/j.chemosphere.2023.140648.

American Public Health Association: Washington, DC, USA, 2005. APHA; AWWA; WEF. Standard Methods for the Examination of Water and Wastewater, 21st ed.

Angulo, E., 1996. The Tomlinson pollution load index applied to heavy metal, ‘MusselWatch’ data: a useful index to assess coastal pollution. Sci. Total Environ. 187, 19–56. https://doi.org/10.1016/0048-9697(96)05128-5.

Ashton, K., Holmes, L., Turner, A., 2010. Association of metals with plastic production pellets in the marine environment. Mar. Pollut. Bull. 60, 2050–2055. https://doi.org/10.1016/j.marpolbul.2010.07.014.

Baresel, C., Olshammar, M., 2019. On the importance of sanitary sewer overflow on the Total discharge of microplastics from sewage water. J. Environ. Prot. 10, 1105–1118. https://www.scirp.org/journal/jep.

Bartoletti, A., Barker, R., Chelazzi, D., Bonelli, N., Baglioni, P., Lee, J., Angelova, L.V., Ormsby, B., 2020. Reviving WHAAM! A comparative evaluation of cleaning systems for the conservation treatment of Roy Lichtenstein’s iconic painting. Herit. Sci. 8, 9. https://doi.org/10.1186/s40494-020-0350-2.

Blair, R.M., Waldron, S., Gauchotte-Lindsay, C., 2019. Average daily flow of microplastics through a tertiary wastewater treatment plant over a ten-month period. Water Res. 163, 114909 https://doi.org/10.1016/j.watres.2019.114909.

Bollmann, U.E., Simon, M., Vollertsen, J., Bester, K., 2019. Assessment of input of organic micropollutants and microplastics into the Baltic Sea by urban waters. Mar. Pollut. Bull. 148, 149–155. https://doi.org/10.1016/j.marpolbul.2019.07.014.

Botturi, A., Ozbayram, E.G., Tondera, K., Gilbert, N.I., Rouault, P., Caradot, N., Gutierrez, O., Daneshgar, S., Frison, N., Akyol, Ç., Foglia, A., 2021. Combined sewer overflows: a critical review on best practice and innovative solutions to mitigate impacts on environment and human health. Environ. Sci. Technol. 51, 1585–1618. https://doi.org/10.1080/10643389.2020.1757957.

Brennecke, D., Duarte, B., Paiva, F., Caçador, I., Canning-Clode, J., 2016. Microplastics as vector for heavy metal contamination from the marine environment. Estuar. Coast. Shelf Sci. 178, 189–195. https://doi.org/10.1016/j.ecss.2015.12.003.

Bydalek, F., Ifayemi, D., Reynolds, L., Barden, R., Kasprzyk-Hordern, B., Wenk, J., 2023. Microplastic dynamics in a free water surface constructed wetland. Sci. Total Environ. 858, 160113 https://doi.org/10.1016/j.scitotenv.2022.160113.

Castillo, A.B., El-Azhary, M., Sorino, C., LeVay, L., 2024. Potential ecological risk assessment of microplastics in coastal sediments: their metal accumulation and interaction with sedimentary metal concentration. Sci. Total Environ. 906, 167473 https://doi.org/10.1016/j.scitotenv.2023.167473.

Chen, H., Jia, Q., Zhao, X., Li, L., Nie, Y., Liu, H., Ye, J., 2020. The occurrence of microplastics in water bodies in urban agglomerations: impacts of drainage system overflow in wet weather, catchment land-uses, and environmental management practices. Water Res. 183, 116073 https://doi.org/10.1016/j.watres.2020.116073.

Chen, Y., Li, T., Hu, H., Ao, H., Xiong, X., Shi, H., Wu, C., 2021. Transport and fate of microplastics in constructed wetlands: a microcosm study. J. Hazard. Mater. 415, 125615 https://doi.org/10.1016/j.jhazmat.2021.125615.

Chen, Z., Hay, J.N., Jenkins, M.J., 2012. FTIR spectroscopic analysis of poly(ethylene terephthalate) on crystallization. Eur. Polym. J. 48, 1586–1610. https://doi.org/10.1016/j.eurpolymj.2012.06.006.

Coates, J., 2006. Interpretation of infrared spectra, a practical approach. Encycl. Anal. Chem. 1–23 https://doi.org/10.1002/9780470027318.a5606.

Dris, R., Gasperi, J., Rocher, V., Saad, M., Renault, N., Tassin, B., 2015. Microplastic contamination in an urban area: a case study in greater Paris. Environ. Chem. 12, 592. https://doi.org/10.1071/EN14167.

Gardette, M., Perthue, A., Gardette, J.L., Janecska, T., Foldes, E., Pukanszky, B., Therias, S., 2013. Photo- and thermal-oxidation of polyethylene: comparison of mechanisms and influence of unsaturation content. Polym. Degrad. Stab. 98, 2383–2390. https://doi.org/10.1016/j.polymdegradstab.2013.07.017.

Haegerbaeumer, A., Mueller, M.T., Fueser, H., Traunspurger, W., 2019. Impacts of microand nano-sized plastic particles on benthic invertebrates: a literature review and gap analysis. Front. Environ. Sci. 7, 17. https://doi.org/10.3389/FENVS.2019.00017.

Hakanson, L., 1980. An ecological risk index for aquatic pollution control. A sedimentological approach. Water Res. 14, 975–1001. https://doi.org/10.1016/0043-1354(80)90143-8.

Hartmann, N.B., Hüffer, T., Thompson, R.C., Hassellov, M., Verschoor, A., Daugaard, A. E., Rist, S., Karlsson, T., Brennholt, N., Cole, M., Herrling, M.P., Hess, M.C., Ivleva, N. P., Lusher, A.L., Wagner, M., 2019. Are we speaking the same language? Recommendations for a definition and categorization framework for plastic debris. Environ. Sci. Technol. 53, 1039–1047. https://doi.org/10.1021/acs.est.8b05297.

Jung, M.R., Horgen, F.D., Orski, S.V., Rodriguez, C.V., Beers, K.L., Balazs, G.H., Jones, T. T., Work, T.M., Brignac, K.C., Royer, S.J., Hyrenbach, K.D., Jensen, B.A., Lynch, J. M., 2018. Validation of ATR FT-IR to identify polymers of plastic marine debris, including those ingested by marine organisms. Mar. Pollut. Bull. 127, 704–716. https://doi.org/10.1016/j.marpolbul.2017.12.061.

Koelmans, A.A., Redondo-Hasselerharm, P.E., Nor, N.H.M., de Ruijter, V.N., Mintenig, S. M., Kooi, M., 2022. Risk assessment of microplastic particles. Nat. Rev. Mater. 7, 138–152. https://doi.org/10.1038/s41578-021-00411-y.

Kutralam-Muniasamy, G., Perez-Guevara, F., Martínez, I.E., Shruti, V., 2021. Overview of microplastics pollution with heavy metals: analytical methods, occurrence, transfer risks and call for standardization. J. Hazard. Mater. 415, 125755 https://doi.org/10.1016/j.jhazmat.2021.125755.

Li, R., Yu, L., Chai, M., Wu, H., Zhu, X., 2020. The distribution, characteristics and ecological risks of microplastics in the mangroves of southern China. Sci. Total Environ. 708, 135025 https://doi.org/10.1016/j.scitotenv.2019.135025.

Lithner, D., Larsson, Å., Dave, G., 2011. Environmental and health hazard ranking and assessment of plastic polymers based on chemical composition. Sci. Total Environ. 409, 3309–3324. https://doi.org/10.1016/j.scitotenv.2011.04.038.

Liu, F., Olesen, K.B., Borregaard, A.R., Vollertsen, J., 2019a. Microplastics in urban and highway stormwater retention ponds. Sci. Total Environ. 671, 992–1000. https://doi.org/10.1016/j.scitotenv.2019.03.416.

Liu, K., Wang, X., Fang, T., Xu, P., Zhu, L., Li, D., 2019b. Source and potential risk assessment of suspended atmospheric microplastics in Shanghai. Sci. Total Environ. 675, 462–471. https://doi.org/10.1016/j.scitotenv.2019.04.110.

Liu, S., Zhao, Y., Li, T., Hu, T., Zheng, K., Shen, M., Long, H., 2023. Removal of micro/nanoplastics in constructed wetland: efficiency, limitations and perspectives. J. Chem. Eng. 475, 146033 https://doi.org/10.1016/j.cej.2023.146033.

Long, Z., Pan, Z., Wang, W., Ren, J., Yu, X., Lin, L., Lin, H., Chen, H., Jin, X., 2019. Microplastic abundance, characteristics, and removal in wastewater treatment plants in a coastal city of China. Water Res. 155, 255–265. https://doi.org/10.1016/j.watres.2019.02.028.

Lu, H.-C., Ziajahromi, S., Locke, A., Neale, P.A., Leusch, F.D.L., 2022. Microplastics profile in constructed wetlands: distribution, retention and implications. Environ. Pollut. 313, 120079 https://doi.org/10.1016/j.envpol.2022.120079.

Luo, H., Luo, L., Huang, G., Liu, P., Li, J., Hu, S., Wang, F., Xu, R., Huang, X., 2009. Total pollution effect of urban surface runoff. J. Environ. Sci. 21, 1186–1193. https://doi.org/10.1016/S1001-0742(08)62402-X.

Mak, C.W., Tsang, Y.Y., Leung, M.M.L., Fang, J.K.H., Chan, K.M., 2020. Microplastics from effluents of sewage treatment works and stormwater discharging into the

Victoria Harbor. Hong Kong. Mar. Pollut. Bull. 157, 111181 https://doi.org/10.1016/j.marpolbul.2020.111181.
Mamun, A.A., Shams, S., Nuruzzaman, M., 2020. Review on uncertainty of the first-flush phenomenon in diffuse pollution control. Appl Water Sci 10, 53. https://doi.org/10.1007/s13201-019-1127-1.
Masi, F., Bresciani, R., Rizzo, A., Conte, G., 2017. Constructed wetlands for combined sewer overflow treatment: ecosystem services at Gorla Maggiore. Italy. Ecol. Eng. 98, 427–438. https://doi.org/10.1016/j.ecoleng.2016.03.043.
Masi, F., Sarti, C., Cincinelli, A., Bresciani, R., Martinuzzi, N., Bernasconi, M., Rizzo, A., 2023. Constructed wetlands for the treatment of combined sewer overflow upstream of centralized wastewater treatment plants. Ecol. Eng. 193, 107008 https://doi.org/10.1016/j.ecoleng.2023.107008.
Massos, A., Turner, A., 2017. Cadmium, lead and bromine in beached microplastics. Environ. Pollut. 227, 139–145. https://doi.org/10.1016/j.envpol.2017.04.034.
Pan, Z., Liu, Q., Jiang, R., Li, W., Sun, X., Lin, H., Jiang, S., Huang, H., 2021. Microplastic pollution and ecological risk assessment in an estuarine environment: the Dongshan Bay of China. Chemosphere 262, 127876. https://doi.org/10.1016/j.chemosphere.2020.127876 0045-6535.
Patterson, J., Jeyasanta, K.I., Sathish, N., Edward, J.P., Booth, A.M., 2020. Microplastic and heavy metal distributions in an Indian coral reef ecosystem. Sci. Total Environ. 744, 140706 https://doi.org/10.1016/j.scitotenv.2020.140706.
Pereira, L.C.C., Dias, J.A., do Carmo, J.A., Polette, M., 2009. Prefacio: A Zona Costeira Amazonica Brasileira. Rev. Gestao Costeira Integr. 9, 3–7. https://doi.org/10.5894/rgci172.
Perry, W.B., Ahmadian, R., Munday, M., Jones, O., Ormerod, S.J., Durance, I., 2024. Addressing the challenges of combined sewer overflows. Environ. Pollut. 343, 123225 https://doi.org/10.1016/j.envpol.2023.123225.
Petrie, B., 2021. A review of combined sewer overflows as a source of wastewater-derived emerging contaminants in the environment and their management. Environ. Sci. Pollut. Res. 28, 32095–32110. https://doi.org/10.1007/s11356-021-14103-1.
Pistocchi, A., Dorati, C., Grizzetti, B., Udias, A., Vigiak, O., Zanni, M., 2019. Water quality in Europe: Effects of the urban wastewater treatment directive. A retrospective and scenario analysis of Dir. In: 91/271/EEC, EUR 30003 EN. Publications Office of the European Union, Luxembourg. https://doi.org/10.2760/303163, 978-92-76-11263-1.
Polanco, H., Hayesa, S., Roblea, C., Krupitskya, M., Brancob, B., 2020. The presence and significance of microplastics in surface water in the lower Hudson River estuary 2016–2019: a research note. Mar. Pollut. Bull. 161, 111702 https://doi.org/10.1016/j.marpolbul.2020.111702.
Qian, J., Tang, S., Wang, P., Lu, B., Li, K., Jin, W., He, X., 2021. From source to sink: review and prospects of microplastics in wetland ecosystems. Sci. Total Environ. 758, 143633 https://doi.org/10.1016/j.scitotenv.2020.143633.
Quaranta, E., Fuchs, S., Liefting, H.J., Schellart, A., Pistocchi, A., 2022a. Costs and benefits of combined sewer overflow management strategies at the European scale. J. Environ. Manag. 318, 115629 https://doi.org/10.1016/j.jenvman.2022.115629.
Quaranta, E., Fuchs, S., Liefting, H.J., Schellart, A., Pistocchi, A., 2022b. A hydrological model to estimate pollution from combined sewer overflows at the regional scale. Application to Europe. J. Hydrol. Reg. Stud., 41, 101080. doi:https://doi.org/10.1016/j.ejrh.2022.101080.
Ranjani, M., Veerasingam, S., Venkatachalapathy, R., Jinoj, T.P.S., Guganathan, L., Mugilarasan, M., Vethamony, P., 2022. Seasonal variation, polymer hazard risk and controlling factors of microplastics in beach sediments along the southeast coast of India. Environ. Pollut. 305, 119315 https://doi.org/10.1016/j.envpol.2022.119315.
Rathore, C., Saha, M., Gupta, P., Kumar, M., Naik, A., de Boer, J., 2023. Standardization of micro-FTIR methods and applicability for the detection and identification of microplastics in environmental matrices. Sci. Total Environ. 888, 164157 https://doi.org/10.1016/j.scitotenv.2023.164157.
Rizzo, A., Bresciani, R., Masi, F., Boano, F., Revelli, R., Ridolfi, L., 2018. Flood reduction as an ecosystem service of constructed wetlands for combined sewer overflow. J. Hydrol. 560, 150–159. https://doi.org/10.1016/j.jhydrol.2018.03.020.
Rizzo, A., Tondera, K., Pálfy, T.G., Dittmer, U., Meyer, D., Schreiber, C., Zacharias, N., Ruppelt, J.P., Esser, D., Molle, P., Troesch, S., Masi, F., 2020. Constructed wetlands for combined sewer overflow treatment: a state-of-the-art review. Sci. Total Environ. 727, 138618 https://doi.org/10.1016/j.scitotenv.2020.138618.
Rizzo, A., Conte, G., Masi, F., 2021. Adjusted unit value transfer as a tool for raising awareness on ecosystem services provided by constructed wetlands for water pollution control: an Italian case study. Int. J. Environ. Res. Public Health 18, 1531. https://doi.org/10.3390/ijerph18041531.
Rose, D., Webber, M., 2019. Characterization of microplastics in the surface waters of Kingston harbour. Sci. Total Environ. 664, 753–760. https://doi.org/10.1016/j.scitotenv.2019.01.319.
Saikia, B.J., Parthasarathy, G., 2010. Fourier transform infrared spectroscopic characterization of kaolinite from Assam and Meghalaya. Northeastern India. J. Mod. Phys 1, 206–210. https://doi.org/10.4236/jmp.2010.14031.
Scopetani, C., Chelazzi, D., Martellini, T., Pellinen, J., Ugolini, A., Sarti, C., Cincinelli, A., 2021. Occurrence and characterization of microplastic and mesoplastic pollution in the Migliarino san Rossore, Massaciuccoli Nature Park (Italy). Mar. Pollut. Bull. 171, 11271. https://doi.org/10.1016/j.marpolbul.2021.112712.
Shen, M., Hu, T., Huang, W., Song, B., Zeng, G., Zhang, Y., 2021. Removal of microplastics from wastewater with aluminosilicate filter media and their surfactant-modified products: performance, mechanism and utilization. Chem. Eng. J. 421, 129918 https://doi.org/10.1016/j.cej.2021.129918.
Singh, S., Kalyanasundaram, M., Diwan, V., 2021. Removal of microplastics from wastewater: available techniques and way forward. Water Sci. Technol. 84, 3689–3704. https://doi.org/10.2166/wst.2021.472.
Sun, X., Jia, Q., Ye, J., Zhu, Y., Song, Z., Guo, Y., Chen, H., 2023. Real-time variabilities in microplastic abundance and characteristics of urban surface runoff and sewer overflow in wet weather as impacted by land use and storm factors. Sci. Total Environ. 859, 160148 https://doi.org/10.1016/j.scitotenv.2022.160148.
Ta, A.T., Babel, S., 2020. Microplastic contamination on the lower Chao Phraya: abundance, characteristic and interaction with heavy metals. Chemosphere 257, 127234. https://doi.org/10.1016/j.chemosphere.2020.127234.
Tomlinson, D.L., Wilson, J.G., Harris, C.R., Jeffrey, D.W., 1980. Problems in the assessment of heavy-metal levels in estuaries and the formation of a pollution index. Helgoländer Meeresun, 33, 566–575. https://link.springer.com/article/10.1007%2FBF02414780.
Tondera, K., 2019. Evaluating the performance of constructed wetlands for the treatment of combined sewer overflows. Ecol. Eng. 137, 53–59. https://doi.org/10.1016/j.ecoleng.2017.10.009.
Wang, C., O'Connor, D., Wang, L., Wu, W.M., Luo, J., Hou, D., 2022. Microplastics in urban runoff: global occurrence and fate. Water Res. 225, 119129 https://doi.org/10.1016/J.WATRES.2022.119129.
Wang, Q., Hernandez-Crespo, C., Santoni, M., Van Hulle, S., Rousseau, D.P.L., 2020. Horizontal subsurface flow constructed wetlands as tertiary treatment: can they be an efficient barrier for microplastics pollution? Sci. Total Environ. 721, 137785 https://doi.org/10.1016/j.scitotenv.2020.137785.
Wang, Q., Hernandez-Crespo, C., Du, B., Van Hulle, S., Rousseau, D., 2021. Fate and removal of microplastics in unplanted lab-scale vertical flow constructed wetlands. Sci. Total Environ. 778, 146152 https://doi.org/10.1016/j.scitotenv.2021.146152.
Wei, L., Yue, Q., Chen, G., Wang, J., 2023. Microplastics in rainwater/stormwater environments: influencing factors, sources, transport, fate, and removal techniques. Trends Anal. Chem. 117147, 117147 https://doi.org/10.1016/j.trac.2023.117147.
Wei, S., Luo, H., Zou, J., Chen, J., Pan, X., Rousseau, D.P.L., Li, J., 2020. Characteristics and removal of microplastics in rural domestic wastewater treatment facilities of China. Sci. Total Environ. 739, 139935 https://doi.org/10.1016/j.scitotenv.2020.139935.
Xu, D., Yin, X., Zhou, S., Jiang, Y., Xi, X., Sun, H., Wang, J., 2022. A review on the remediation of microplastics using constructed wetlands: bibliometric, co-occurrence, current trends, and future directions. Chemosphere 303, 134990. https://doi.org/10.1016/j.chemosphere.2022.134990.
Xu, P., Peng, G., Su, L., Gao, Y., Gao, L., Li, D., 2018. Microplastic risk assessment in surface waters: a case study in the Changjiang Estuary, China. Mar. Pollut. Bull. 133, 647e654. https://doi.org/10.1016/j.marpolbul.2018.06.020.
Yu, D., Dian, L., Hai, Y., Randall, M.T., Liu, L., Liu, J., Zhang, J., Zheng, X., Wei, Y., 2022. Effect of rainfall characteristics on the sewer sediment, hydrograph, and pollutant discharge of combined sewer overflow. J. Environ. Manag. 303, 114268 https://doi.org/10.1016/j.jenvman.2021.114268.
Zambrano, M.C., Pawlak, J.J., Daystar, J., Ankeny, M., Venditti, R.A., 2021. Impact of dyes and finishes on the aquatic biodegradability of cotton textile fibers and microfibers released on laundering clothes: correlations between enzyme adsorption and activity and biodegradation rates. Mar. Pollut. Bull. 165, 112030 https://doi.org/10.1016/j.marpolbul.2021.112030.
Zha, F., Shang, M., Ouyang, Z., Guo, X., 2022. The aging behaviors and release of microplastics: a review. Gondwana Res. 108, 60–71. https://doi.org/10.1016/j.gr.2021.10.025.
Zhang, C.F., Zhou, H.H., Cui, Y.Z., Wang, C.S., Li, Y.J., Zhang, D.D., 2019. Microplastics in offshore sediment in the Yellow Sea and East China Sea. China. Environ. Pollut. 244, 827–833. https://doi.org/10.1016/j.envpol.2018.10.102.
Zhou, X., Zhao, Y., Pang, G., Jia, X., Song, Y., Guo, A., Wang, A., Zhang, S., Ji, M., 2022. Microplastic abundance, characteristics and removal in large-scale multi-stage constructed wetlands for effluent polishing in northern China. J. Chem. Eng. 430, 132752 https://doi.org/10.1016/j.cej.2021.132752.
Zhou, Y., Li, Y., Yan, Z., Wang, H., Chen, H., Zhao, S., Zhong, N., Cheng, Y., Acharya, K., 2023. Microplastics discharged from urban drainage system: prominent contribution of sewer overflow pollution. Water Res. 236, 119976 https://doi.org/10.1016/j.watres.2023.119976.